

# **A correlation for the lift-off of many particles in plane Poiseuille flows of Newtonian fluids**

N.A. Patankar<sup>1#</sup>, T. Ko<sup>1</sup>, H.G. Choi<sup>2</sup> and D.D. Joseph<sup>1</sup>

<sup>1</sup>Department of Aerospace Engineering and Mechanics and the Minnesota Supercomputer Institute,  
University of Minnesota, Minneapolis, MN 55455, USA

<sup>2</sup>School of Mechanical and Aerospace Engineering,  
Seoul National University, Seoul 151-742, South Korea

## **Abstract**

Choi & Joseph (2001) reported a two-dimensional numerical investigation of the lift-off of 300 circular particles in plane Poiseuille flows of Newtonian fluids. We perform similar simulations. Particles heavier than the fluid are initially placed in a closely packed ordered configuration at the bottom of a periodic channel. The fluid-particle mixture is driven by an external pressure gradient. The particles are suspended or fluidized by lift forces that balance the buoyant weight perpendicular to the flow. Pressure waves corresponding to the waves at the fluid-mixture interface are observed. During the initial transient, these waves grow, resulting in bed erosion. At sufficiently large shear Reynolds numbers the particles occupy the entire channel width during the transient. The particle bed eventually settles to an equilibrium height which increases as the shear Reynolds number is increased. Heavier particles are lifted to a smaller equilibrium height at the same Reynolds number. A correlation for the lift-off of many particles is obtained from the numerical data. The correlation is used to estimate the critical shear Reynolds number for lift-off of many particles. The critical shear Reynolds number for lift-off of a single particle is found to be greater than that for many particles. The procedures used here to obtain correlations from direct simulations in 2D and the type of correlations that emerge should generalize to 3D simulations presently underway.

---

<sup>#</sup> Current address: Department of Mechanical Engineering, Northwestern University, Evanston, IL 60208

## 1. Introduction

Lift plays a central role in the suspension of particles in the flow of slurries. In the oil industry we can consider the removal of drill cuttings in horizontal drill holes and sand (or proppant) transport in fractured reservoirs. A force experienced by a particle moving through a fluid with circulation (or shearing motion for a viscous fluid) is referred to as the lift force in the present work.

Modeling of solid-liquid mixtures has been approached in two ways. The first approach is to consider the solid-liquid mixture as an effective fluid medium. Bulk properties (such as the effective viscosity) of the composite mixture are then modeled. In the second approach the solid and the fluid are considered as inter-penetrating mixtures which are governed by conservation laws. Interaction between the inter-penetrating phases is modeled. This is the mixture theory approach. Models for drag and lift forces on the particles must be used in mixture theories. Models for the drag force on particles in solid-liquid mixtures is a complicated issue and usually rely on the well-known Richardson-Zaki (1954) correlation. Models for lift forces in mixtures are much less well developed than models for drag.

Joseph (2001) proposed that ideas analogous to the Richardson-Zaki correlation must come into play in problems of slurries, which are fluidized by lift rather than by drag. Various models for the lift on single particles have been proposed (see e.g. Joseph 2001, N. Patankar, Huang, Ko & Joseph 2001, Ko, N. Patankar & Joseph 2001 and references therein) but the dependence of the lift on solids fraction and other many particle parameters is not known. Direct numerical simulations or experiments can be done to develop a suitable engineering correlation for lift.

Morris & Brady (1998) studied the migration of non-neutrally buoyant spheres in pressure driven flows of Newtonian fluids. They performed Stokesian dynamic simulations of a monolayer of spheres. These studies are valid in the creeping flow limit. In applications such as the transport of slurries or proppants, the effect of Reynolds

number on the lift force is important. Choi & Joseph (2001) (hereafter referred to as CJ) reported a two-dimensional numerical investigation of fluidization by lift of 300 circular particles in a Poiseuille flow of a Newtonian fluid. Their results are valid at finite shear Reynolds numbers. They observed that the fluidization of circular particles first involves bed inflation in which liquid is driven into the bed. The bed inflation was observed even at very low shear Reynolds numbers but it took more time for the bed to inflate as the Reynolds number was reduced. Pressure waves corresponding to the waves at the fluid-mixture interface were observed. CJ used a Chorin (1968) type fractional-step scheme developed by Choi (2000) to perform the numerical simulations. We use the same numerical method for the simulations reported in this paper. This method is closely related to the Arbitrary-Lagrangian-Eulerian (ALE) numerical method, using body-fitted unstructured finite element grids to simulate particulate flows, reported by Hu, Joseph & Crochet (1992), Hu (1996), Hu & N. Patankar (2001) and Hu, N. Patankar & Zhu (2001). In these simulations the distance between the particles cannot be equal to zero. We have a small zone around each particle, which we call the security zone. Overlap of the security zones gives rise to a repulsive force that keeps the particles apart.

In this paper an engineering type correlation for the lift-off of many particles is obtained using the numerical data from our simulations and from the simulations of CJ. We also study the effect of various parameters on the flow features. Both the transient and the steady state behavior will be discussed.

The governing equations, various parameters of the problem and a discussion of the lift models for solid-liquid flows will be presented in section 2. Results will be presented in section 3 and conclusions in section 4.

## 2. Governing equations and the parameters of the problem

The two-dimensional computational domain for our simulations is shown in Figure 1. We perform simulations in a periodic domain (Figure 2). The applied pressure gradient is given by  $-\bar{p}$ , where  $\bar{p}$  is considered to be positive.

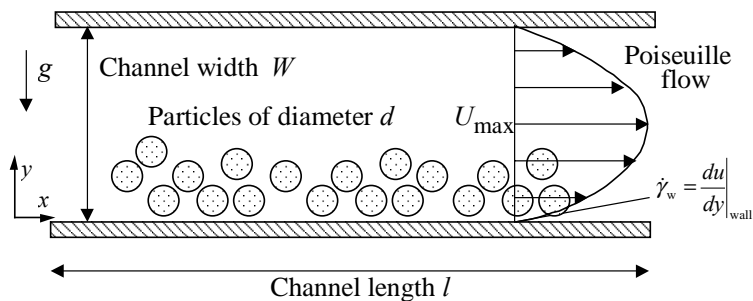


Figure 1. Computational domain for the numerical simulation of lift-off of particles in a plane Poiseuille flow. The wall shear rate  $\dot{\gamma}_w$  is calculated from the parabolic velocity profile in the absence of the particles.

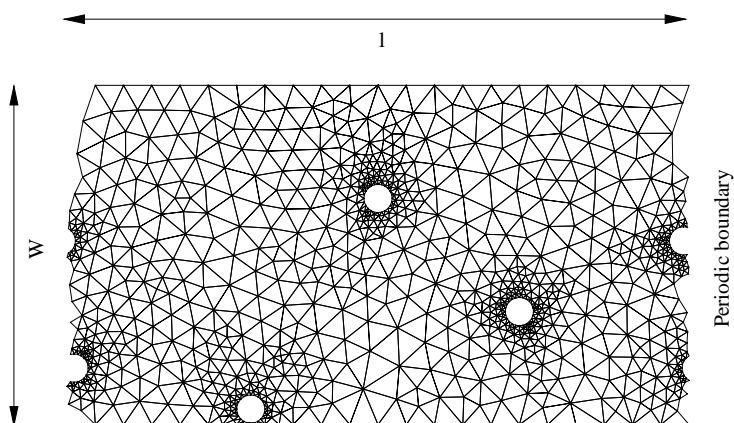


Figure 2. Unstructured mesh in a periodic domain.

We split the pressure as follows:

$$\begin{aligned} P &= p + \rho_f \mathbf{g} \cdot \mathbf{x} - \bar{p} \mathbf{e}_x \cdot \mathbf{x} \\ \Rightarrow -\nabla P &= -\nabla p - \rho_f \mathbf{g} + \bar{p} \mathbf{e}_x \end{aligned} \quad (1)$$

where  $P(\mathbf{x}, t)$  is the total fluid pressure,  $\rho_f$  is the fluid density,  $\mathbf{g}$  is the acceleration due to gravity,  $\mathbf{x}$  is the position vector and  $\mathbf{e}_x$  is the unit vector in the  $x$ -direction. We solve for the ‘dynamic’ pressure  $p$  in our simulations. The external pressure gradient term then

appears as a body force like term in the fluid and particle equations (3). The value of  $\bar{p}$  is specified during the simulations.

The particles are free to rotate and translate. Particles heavier than the fluid are initially placed in a closely packed ordered configuration at the bottom of the channel. Gravity acts in the negative y-direction. A parabolic velocity profile corresponding to  $\bar{p}$  is specified in the clear fluid region as the initial condition. This reduces the time of the initial transient significantly. At  $t = 0_+$  the fluid in the channel is driven by an external pressure gradient along the x-direction. The particles are suspended or fluidized by lift forces that balance the buoyant weight perpendicular to the flow.

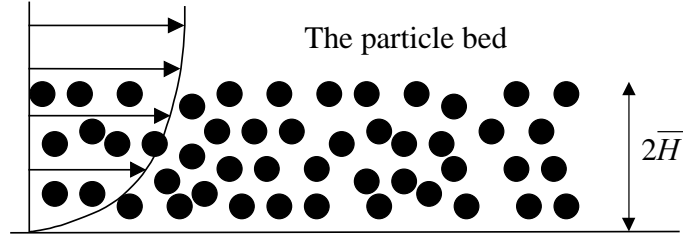


Figure 3. Particles fluidized in a Poiseuille flow.

The average height  $\bar{H}$  of the particle bed reaches an equilibrium value after the initial transient. We define this state as the ‘statistical steady state’. The average height represents the height of the center of gravity of the bed if the distribution of the particles in the bed is uniform. The average fluid fraction  $\varepsilon$  of the bed is given by

$$\varepsilon = 1 - \frac{N\pi d^2}{8\bar{H}l}, \quad (2)$$

where  $N$  is the number of particles in the domain and  $d$  is the diameter of the particles.

The governing equations in non-dimensional form are:

$$\begin{aligned}
 & \left. \begin{aligned}
 & \nabla \cdot \mathbf{u} = 0, \\
 & R \left( \frac{\partial \mathbf{u}}{\partial t} + (\mathbf{u} \cdot \nabla) \mathbf{u} \right) = -\nabla p + 2 \frac{d}{W} \mathbf{e}_x + \nabla \cdot \mathbf{T}, \\
 & \mathbf{T} = \mathbf{A},
 \end{aligned} \right\} \text{Fluid} \\
 & \left. \begin{aligned}
 & \frac{\rho_p}{\rho_f} R \frac{d\mathbf{U}_p}{dt} = 2 \frac{d}{W} \mathbf{e}_x - \frac{R_G}{R} \mathbf{e}_y + \frac{4}{\pi} \oint [-p\mathbf{1} + \mathbf{T}] \cdot \mathbf{n} d\Gamma, \\
 & \frac{\rho_p}{\rho_f} R \frac{d\mathbf{\Omega}_p}{dt} = \frac{32}{\pi} \oint (\mathbf{x} - \mathbf{X}) \times ([-p\mathbf{1} + \mathbf{T}] \cdot \mathbf{n}) d\Gamma,
 \end{aligned} \right\} \text{Particles}
 \end{aligned} \tag{3}$$

where  $\mathbf{u}(\mathbf{x}, t)$  is the fluid velocity,  $\rho_p$  is the particle density,  $\mathbf{T}$  is the extra-stress tensor,  $\mathbf{A} = (\nabla \mathbf{u} + \nabla \mathbf{u}^T)$  is two times the deformation-rate tensor,  $\mathbf{U}_p$  is the translational velocity of the particle,  $\mathbf{\Omega}_p$  is the angular velocity of the particle,  $\mathbf{I}$  is the particle moment of inertia tensor,  $\mathbf{X}$  is the coordinate of the center of mass of the particle and  $\mathbf{e}_y$  is the unit vector in the  $y$ -direction. We have used  $\mathbf{g} = -g\mathbf{e}_y$ . Equation (3) and the corresponding initial and boundary conditions define an initial boundary value problem that can be solved by direct numerical simulation. The parameters in this problem are:

$$\begin{aligned}
 \varepsilon, & \quad \text{average fluid fraction in the particle bed,} \\
 Nd/l, & \quad \text{number of particles per unit dimensionless length,} \\
 R = \frac{\rho_f V d}{\eta} = \frac{\rho_f \dot{\gamma}_w d^2}{\eta} = \frac{\rho_f W d^2}{2\eta^2} \bar{p}, & \quad \text{shear Reynolds number,} \\
 R_G = \frac{\rho_f V_g d}{\eta} = \frac{\rho_f (\rho_p - \rho_f) g d^3}{\eta^2} & \quad \text{, gravity Reynolds number,} \\
 & \quad = \frac{4\rho_f L d}{\pi\eta^2} \\
 \frac{\bar{p} d^2}{\eta V} = \frac{\bar{p} d}{\eta \dot{\gamma}_w} = 2 \frac{d}{W}, & \quad \text{aspect ratio,} \\
 \frac{\rho_p}{\rho_f}, & \quad \text{density ratio,}
 \end{aligned}$$

where  $V_g = \frac{(\rho_p - \rho_f) g d^2}{\eta}$  is the velocity scale of a particle sedimenting in a viscous fluid and  $L$  is the buoyant weight (or lift) on a particle in the absence of any other particles. The dimensionless channel length  $l/d$ , which is also a parameter of the problem,

is chosen large enough so that the solution is only weakly dependent on its value. A dimensionless description of the governing equations is constructed by introducing the following scales: the particle diameter  $d$  for length,  $V$  for velocity,  $d/V$  for time,  $\eta V/d$  for stress and pressure and  $V/d$  for angular velocity of the particle where  $\eta$  is the viscosity of the fluid. We have chosen  $V = \dot{\gamma}_w d$ , where  $\dot{\gamma}_w$  is the shear-rate at the wall (in the absence of the particles) corresponding to the applied pressure gradient  $\bar{p}$  as shown in Figure 1. In our multi-particle simulations we have  $N = 300$ ,  $\rho_p/\rho_f = 1.01$ ,  $W/d = 12$  and  $l/d = 63$ . We take  $d = 1$  cm,  $\rho_p = 1.01$  g/cc and  $\rho_f = 1$  g/cc.

A gravity parameter  $G$ , which represents the ratio of  $V_g$  and  $V$ , is given by  $R_G/R$ . The ratio  $R/G = d\dot{\gamma}_w^2 / ((\rho_p/\rho_f - 1)g)$ , which measures the ratio of inertia to buoyant weight, is a generalized Froude number.

Assuming the channel length to be long, the gravity Reynolds number at the ‘statistical steady state’ depends on the parameters listed above and

$$\begin{array}{l}
 R_G = f\left(R, \varepsilon, \frac{Nd}{l}, \frac{W}{d}\right) . \\
 \text{Since } \varepsilon_{\max} = 1 - \phi_{\min} = 1 - \frac{\pi(Nd/l)}{4(W/d)}, \\
 \text{it follows that } R_G = f\left(R, \varepsilon, \varepsilon_{\max}, \frac{W}{d}\right),
 \end{array}
 \left. \vphantom{\begin{array}{l} R_G = f\left(R, \varepsilon, \frac{Nd}{l}, \frac{W}{d}\right) . \\ \varepsilon_{\max} = 1 - \phi_{\min} = 1 - \frac{\pi(Nd/l)}{4(W/d)}, \\ R_G = f\left(R, \varepsilon, \varepsilon_{\max}, \frac{W}{d}\right), \end{array}} \right\} \quad (4)$$

where  $\varepsilon_{\max}$  is the maximum possible fluid fraction in the channel and  $\phi_{\min}$  is the corresponding value of the minimum particle fraction. The parameter  $\rho_p/\rho_f$  arises only in the particle acceleration terms in the governing equations (3). At steady state the average acceleration of the particles is zero. Hence  $\rho_p/\rho_f$  is not included as a parameter in (4). However, the effect of  $\rho_p/\rho_f$  can be important in characterizing the transient and the ‘mixing’ behavior of the mixture. In our multi-particle simulations,  $W/d$  and  $Nd/l$  (or  $\varepsilon_{\max}$ ) are fixed. The gravity Reynolds number  $R_G$  is therefore a function of  $R$  and  $\varepsilon$ .

### 3. Results

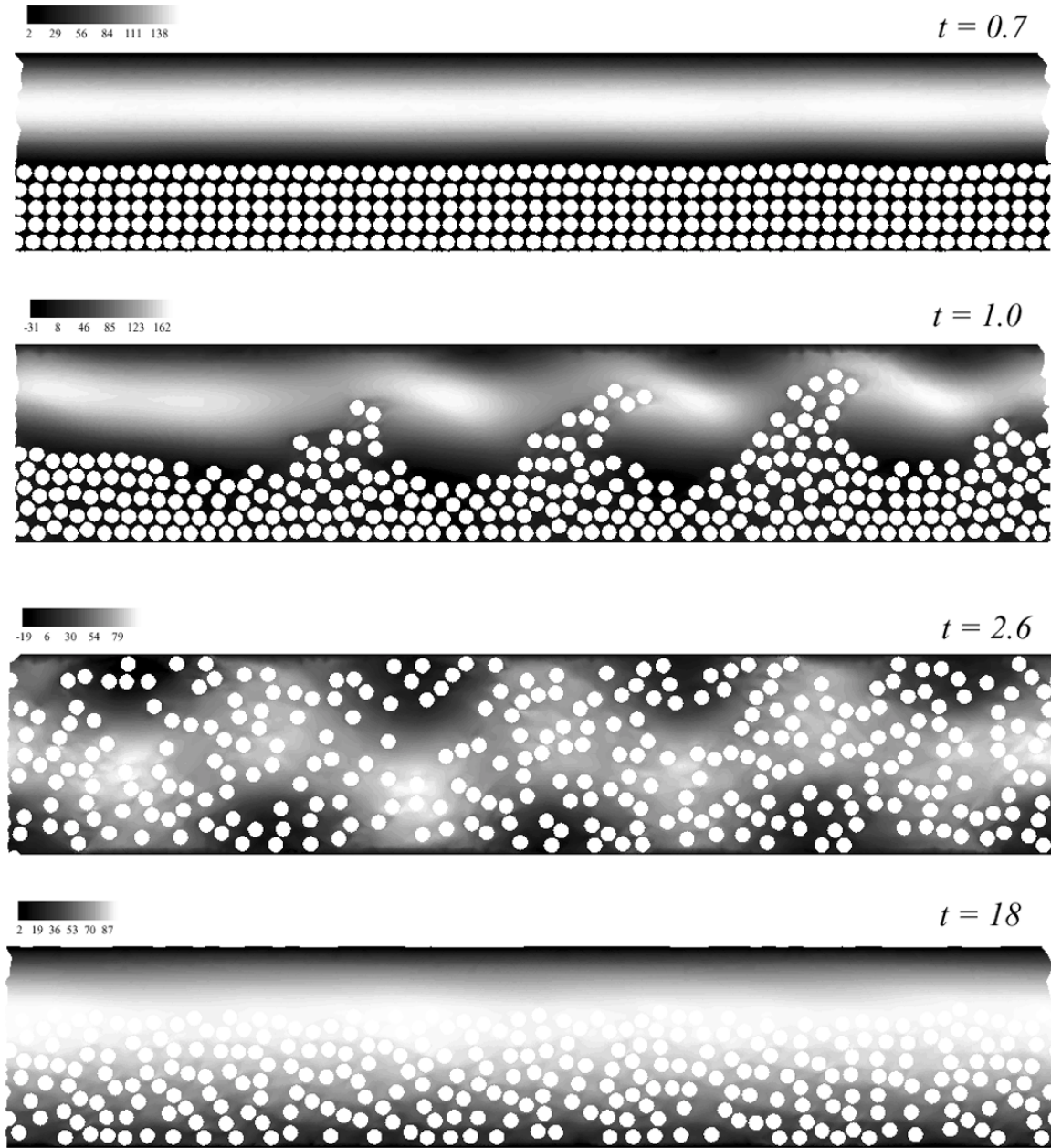
#### 3.1 Numerical simulation of lift-off

The gravity Reynolds number,  $R_G$ , is varied by changing the viscosity of the suspending fluid. For the given choice of parameters,  $R_G = 9.81/\eta^2$ . At a given value of  $R_G$ , the shear Reynolds number  $R$  is varied by changing the applied pressure gradient  $\bar{p}$ . CJ reported simulations with  $\eta = 1$  poise and 0.2 poise. In this paper we perform simulations with  $\eta = 0.1$  poise and 0.05 poise. The primary objective is to obtain more data to develop a correlation for lift.

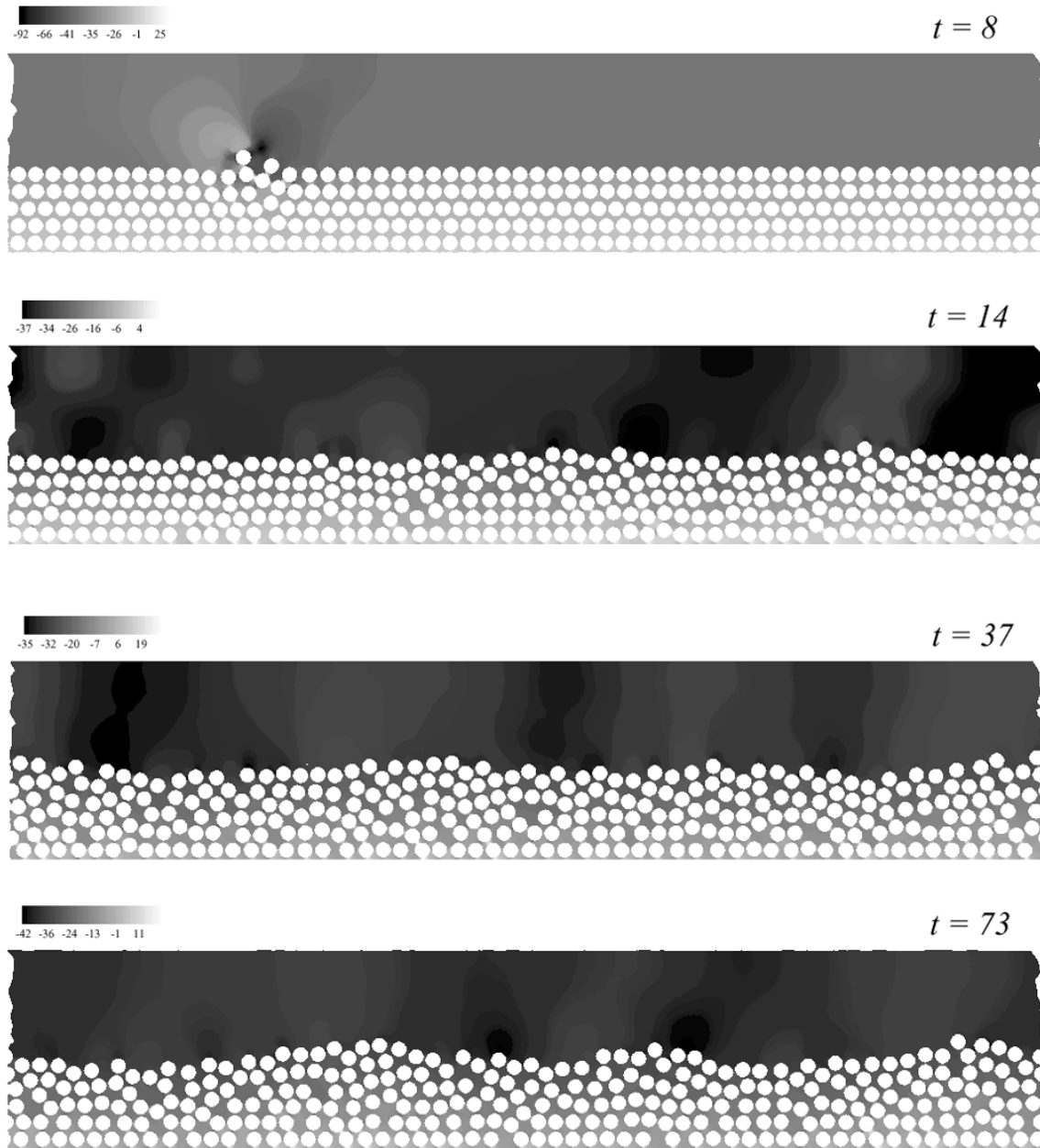
Figure 4 shows the contour plot of the axial velocity for a typical simulation. Snapshots of the pressure distribution for several cases are shown in Figure 5. Light colors indicate high values of pressure. The particles are initially placed in a closely packed ordered configuration. At early times the pressure has vertical stratification. From these figures we observe that the top layer of the particles ‘disturbs’ the flow thus giving rise to regions of high pressure at the front and low pressure at the back of each particle. This disturbance causes a horizontal wave of the dynamic pressure with a periodic length of few particle diameters in the clear fluid region. The fluid-mixture interface forms troughs and crests corresponding to the pressure wave. These interfacial waves, which are more prominent at higher shear Reynolds numbers, grow in amplitude resulting in bed erosion. Similar observation was reported by CJ.

Figure 4 and Figures 5.6, 5.7, 5.12 and 5.13 exhibit intense vortex motion in the early transients prior to the final bed expansion. Drag forces are important in the transients but the final bed height is determined by balance of buoyant weight and lift.





*Figure 4. Lift-off of 300 heavy particles in a plane Poiseuille flow of a Newtonian fluid;  $R = 1800$ ,  $R_G = 981$  and the variables are in CGS units. A contour plot of the horizontal velocity component is shown. Lighter shades indicate higher velocity.*



*Figure 5.1. Fluidization of 300 particles ( $R_G = 981$ ,  $R = 120$ ). The flow is from left to right. The bed height rises slightly.*

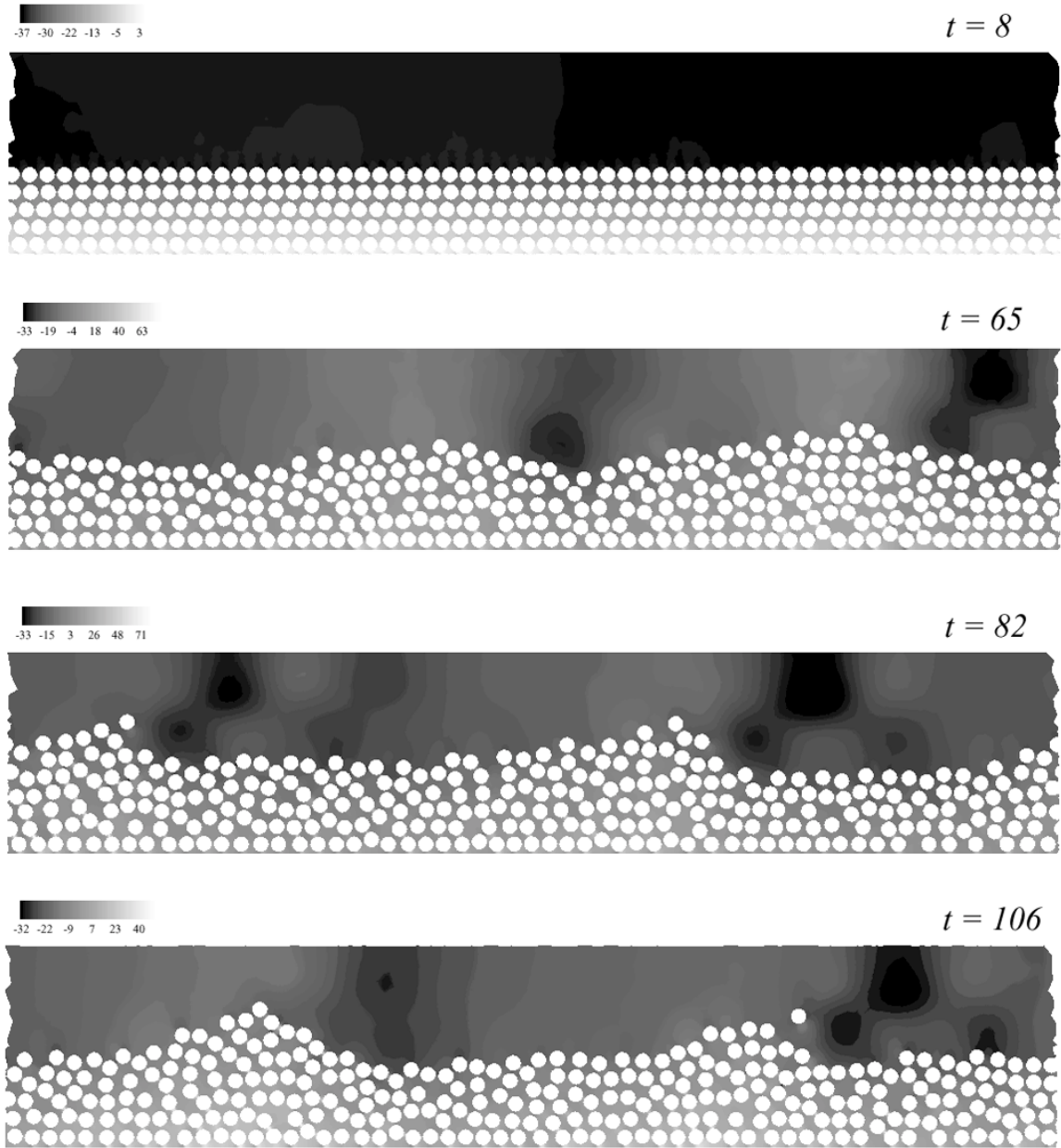


*Figure 5.2. Fluidization of 300 particles ( $R_G = 981$ ,  $R = 180$ ). The bed has eroded more ( $t = 106$  s).*

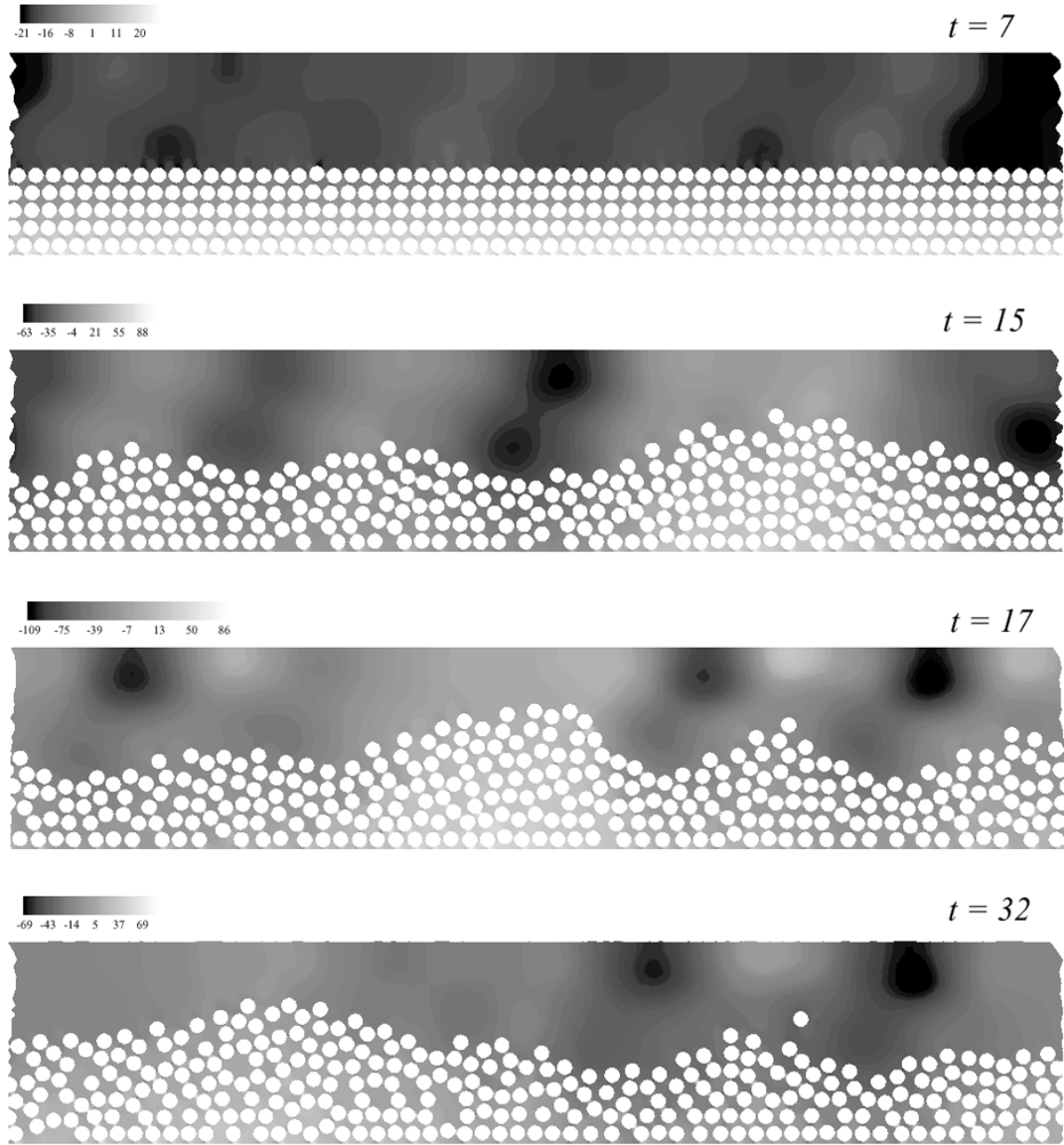
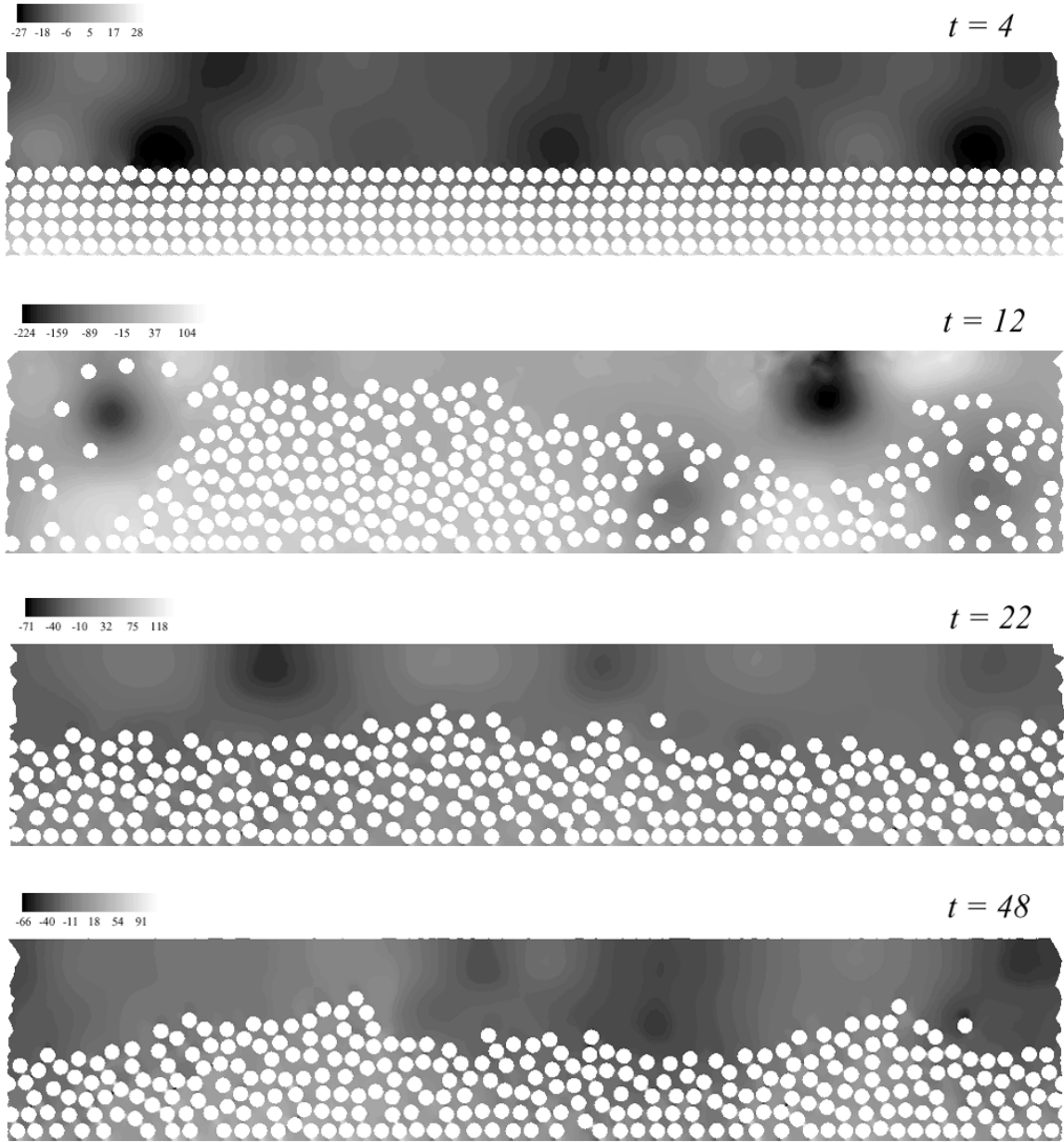


Figure 5.3. Fluidization of 300 particles ( $R_G = 981$ ,  $R = 300$ ).



*Figure 5.4. Fluidization of 300 particles ( $R_G = 981$ ,  $R = 420$ ). The bed height increases with  $R$ .*

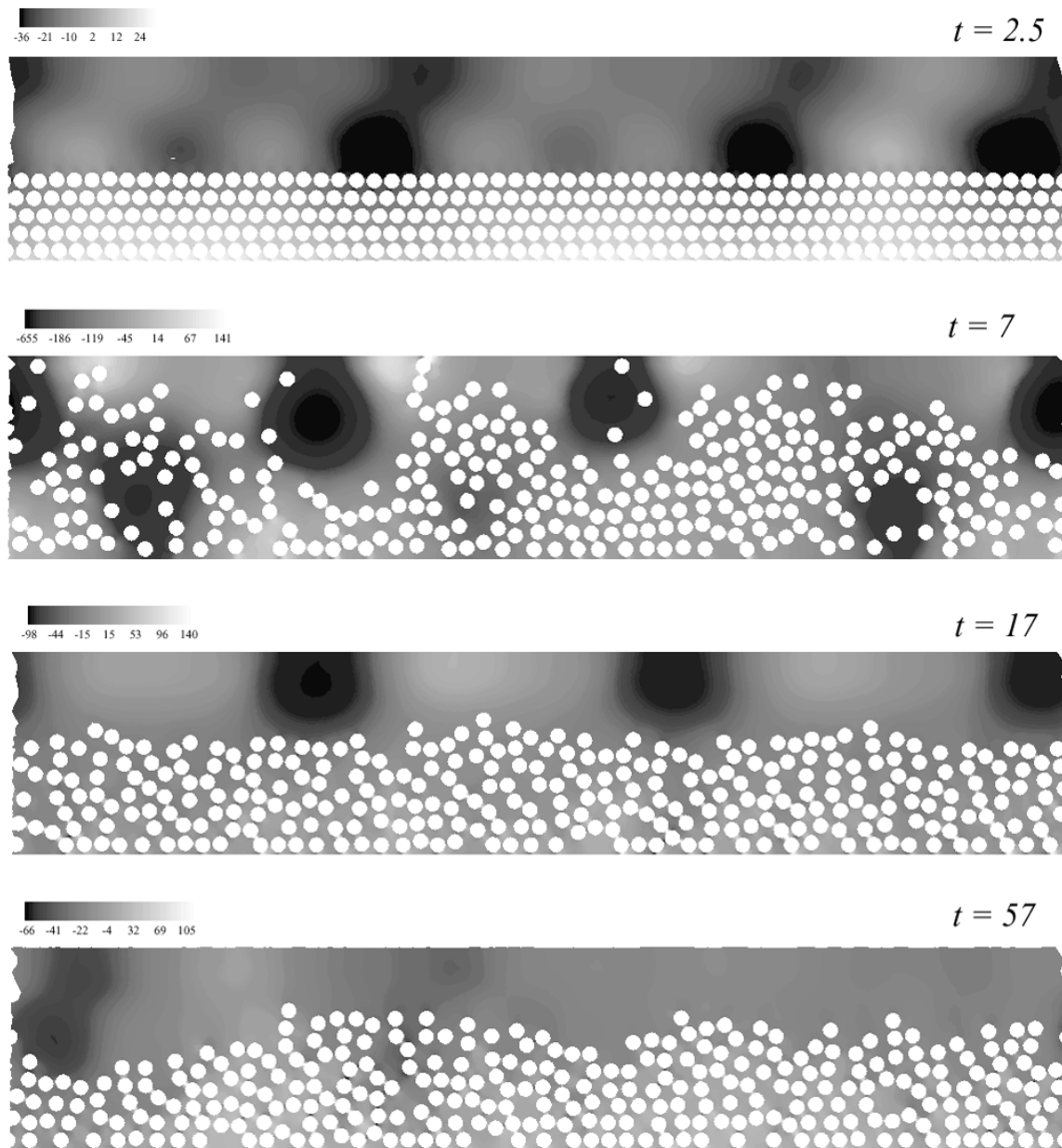
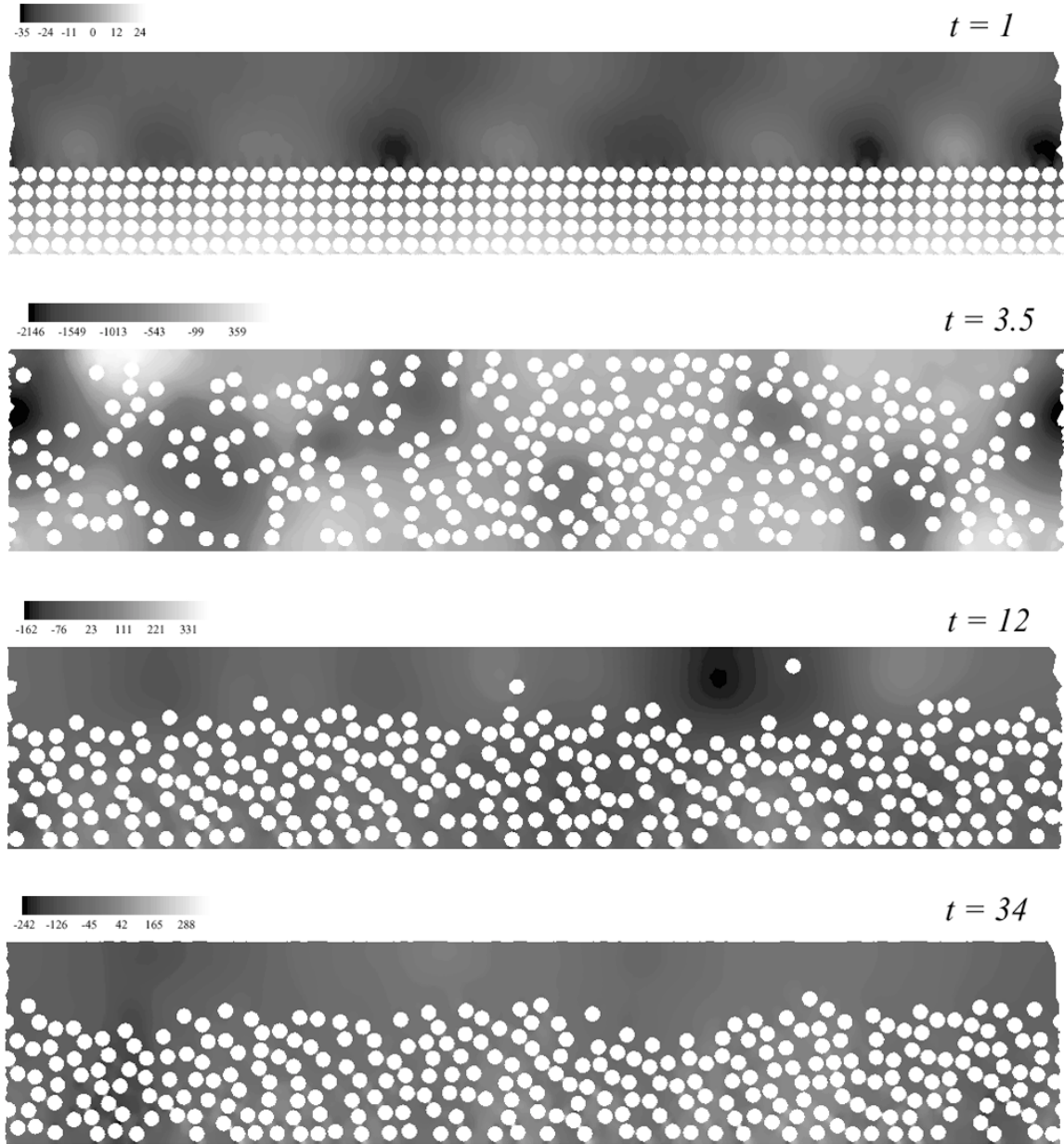
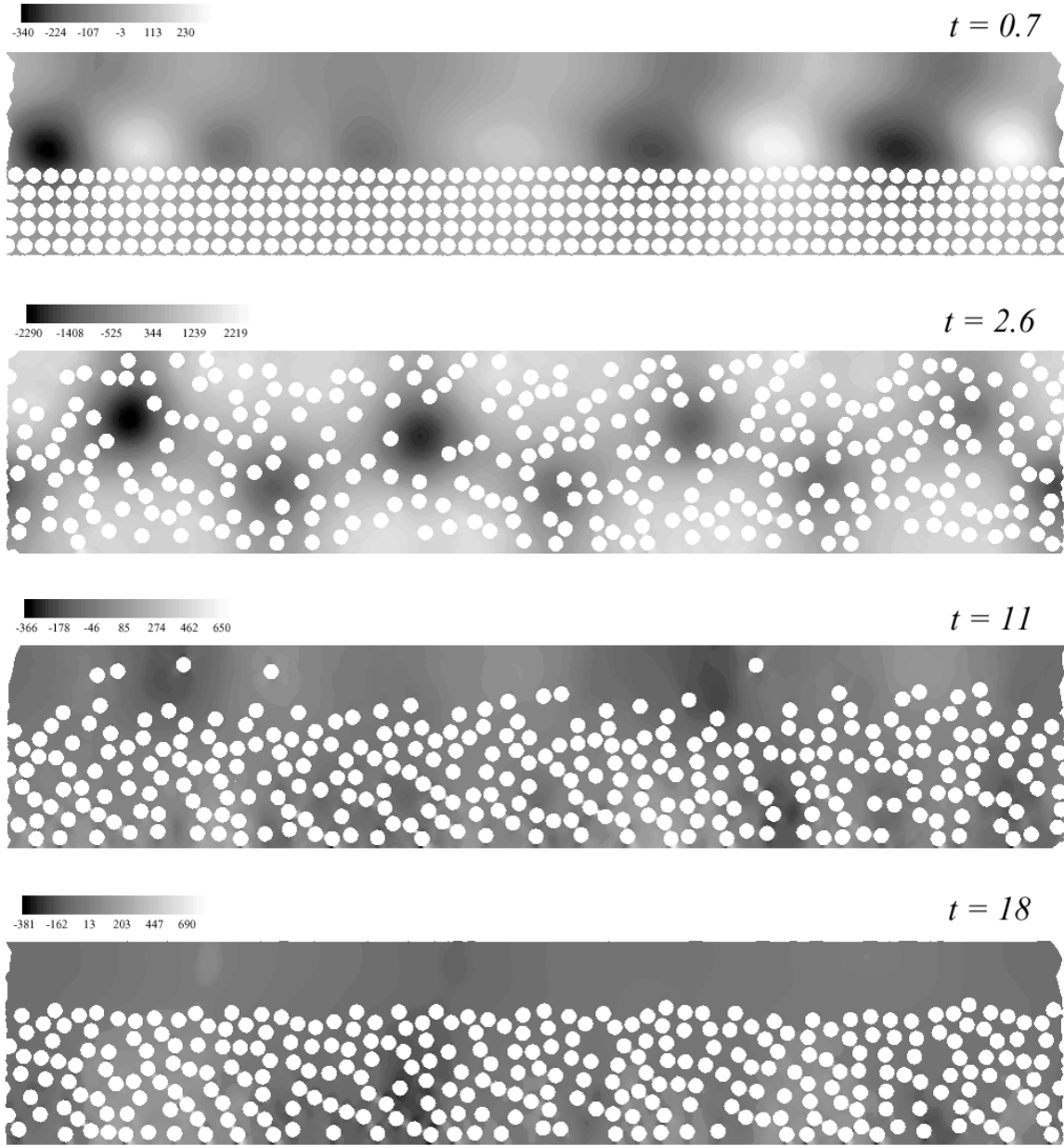


Figure 5.5. Fluidization of 300 particles ( $R_G = 981$ ,  $R = 600$ ).



*Figure 5.6. Fluidization of 300 particles ( $R_G = 981$ ,  $R = 1200$ ). The bed rises at  $t = 3.5$ s to the top wall. The bed settles to its final steady equilibrium height. Interfacial waves corresponding to the pressure waves at the final state are not significant since the particle fraction is not very high.*



*Figure 5.7. Fluidization of 300 particles ( $R_G = 981$ ,  $R = 1800$ ). Interfacial waves at the final state are not significant.*



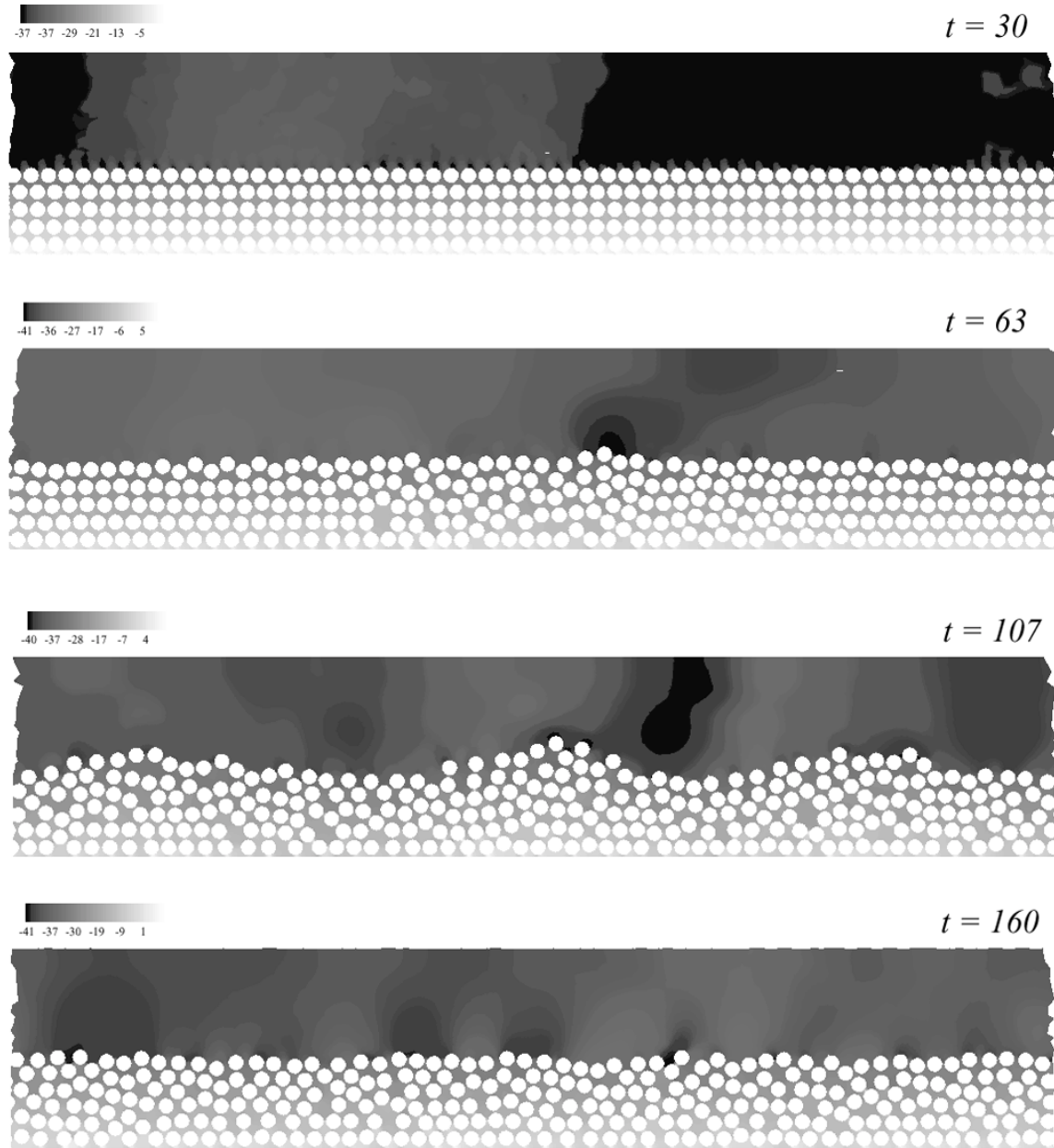


Figure 5.8. Fluidization of 300 particles ( $R_G = 3924$ ,  $R = 240$ ).

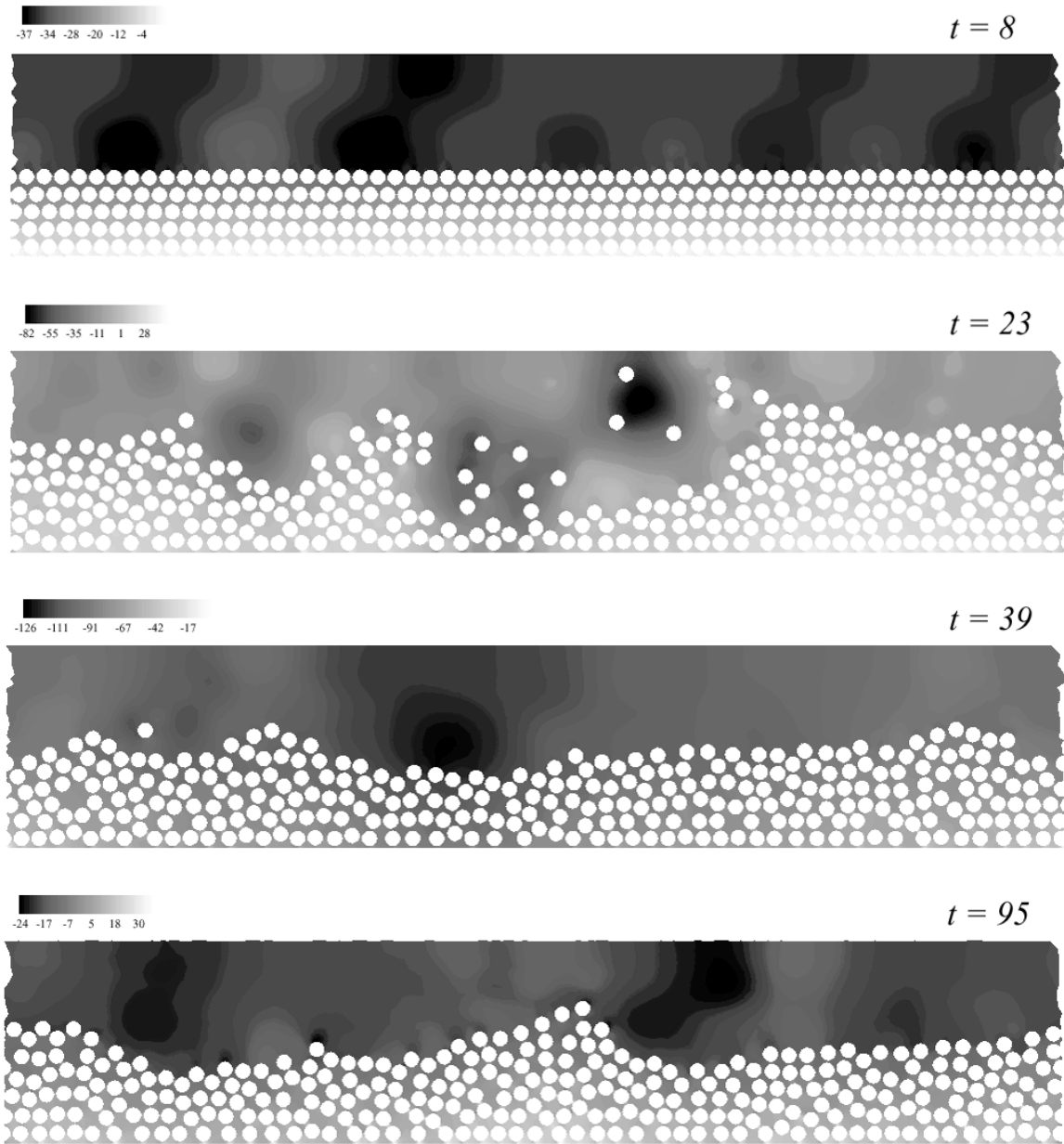


Figure 5.9. Fluidization of 300 particles ( $R_G = 3924$ ,  $R = 480$ ).

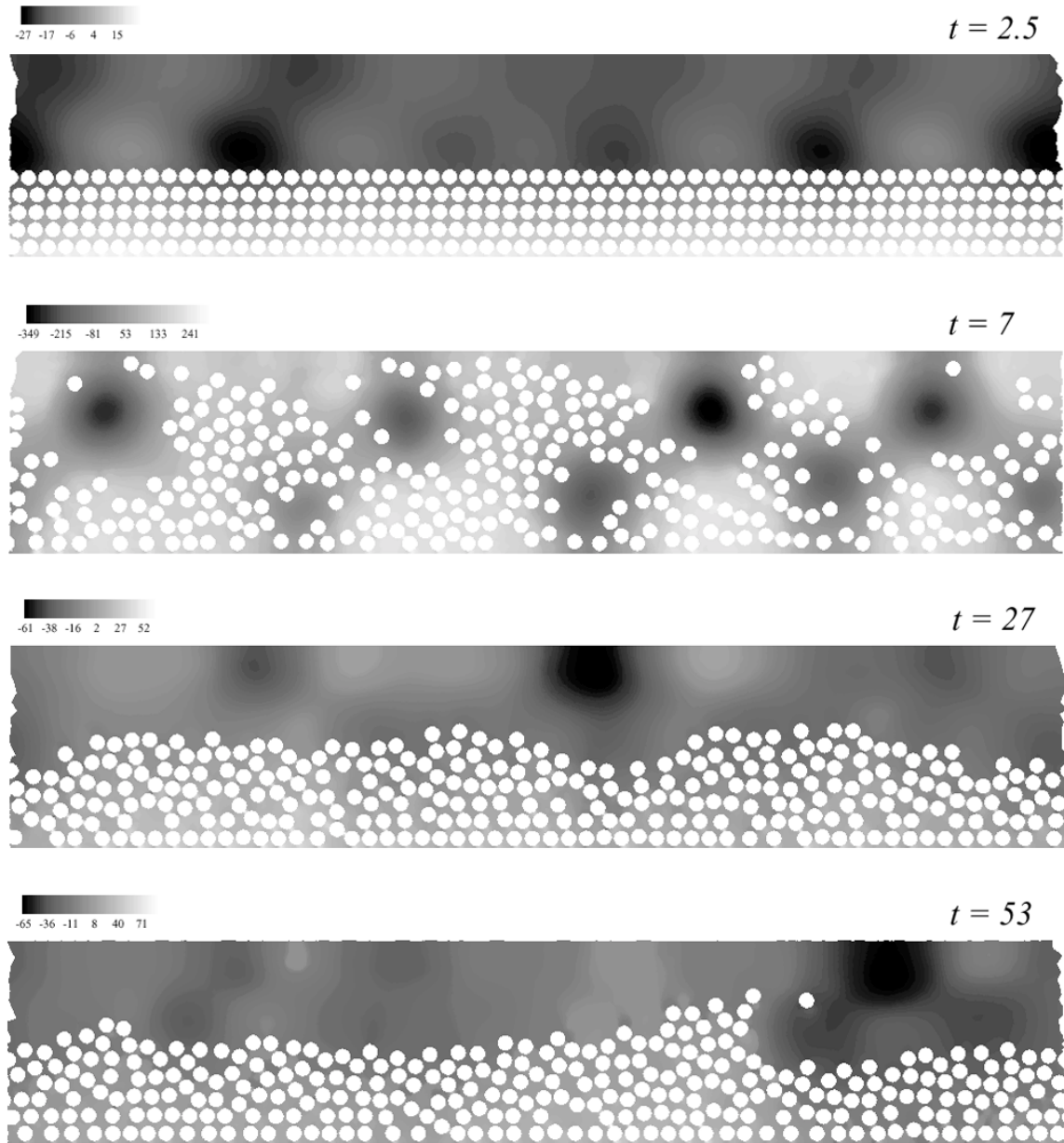


Figure 5.10. Fluidization of 300 particles ( $R_G = 3924$ ,  $R = 960$ ).

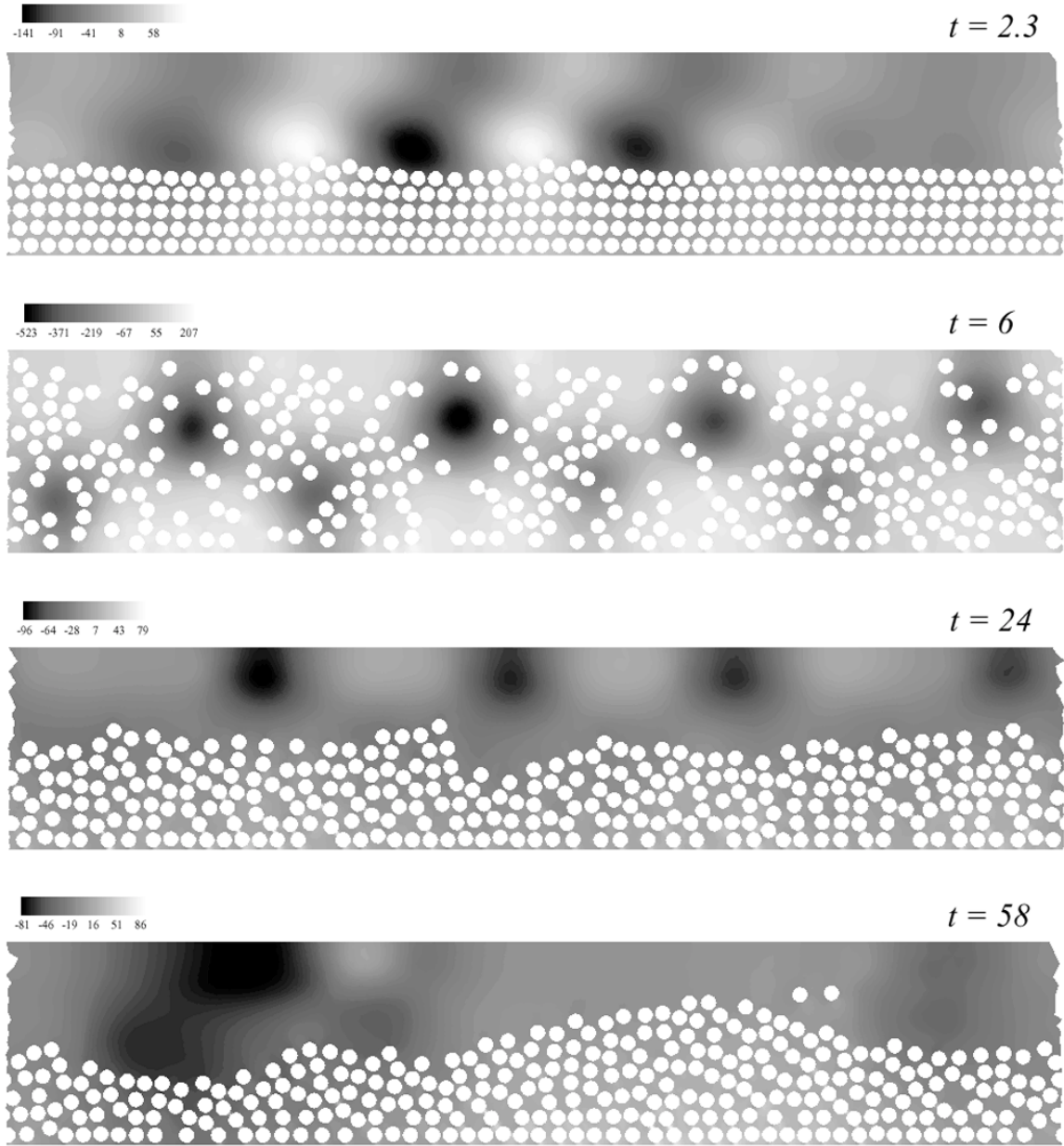


Figure 5.11. Fluidization of 300 particles ( $R_G = 3924$ ,  $R = 1200$ ).

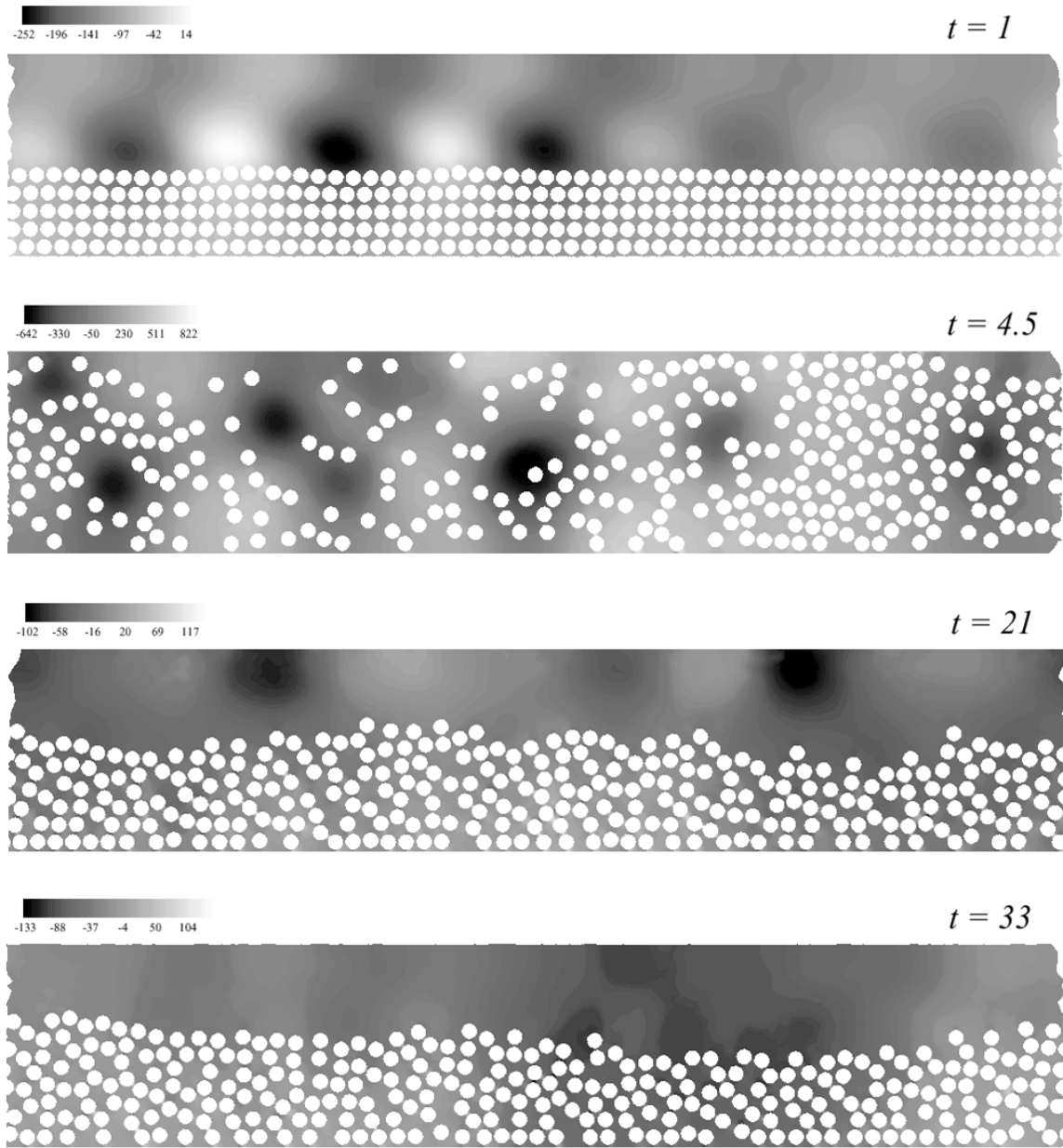


Figure 5.12. Fluidization of 300 particles ( $R_G = 3924$ ,  $R = 1680$ ).

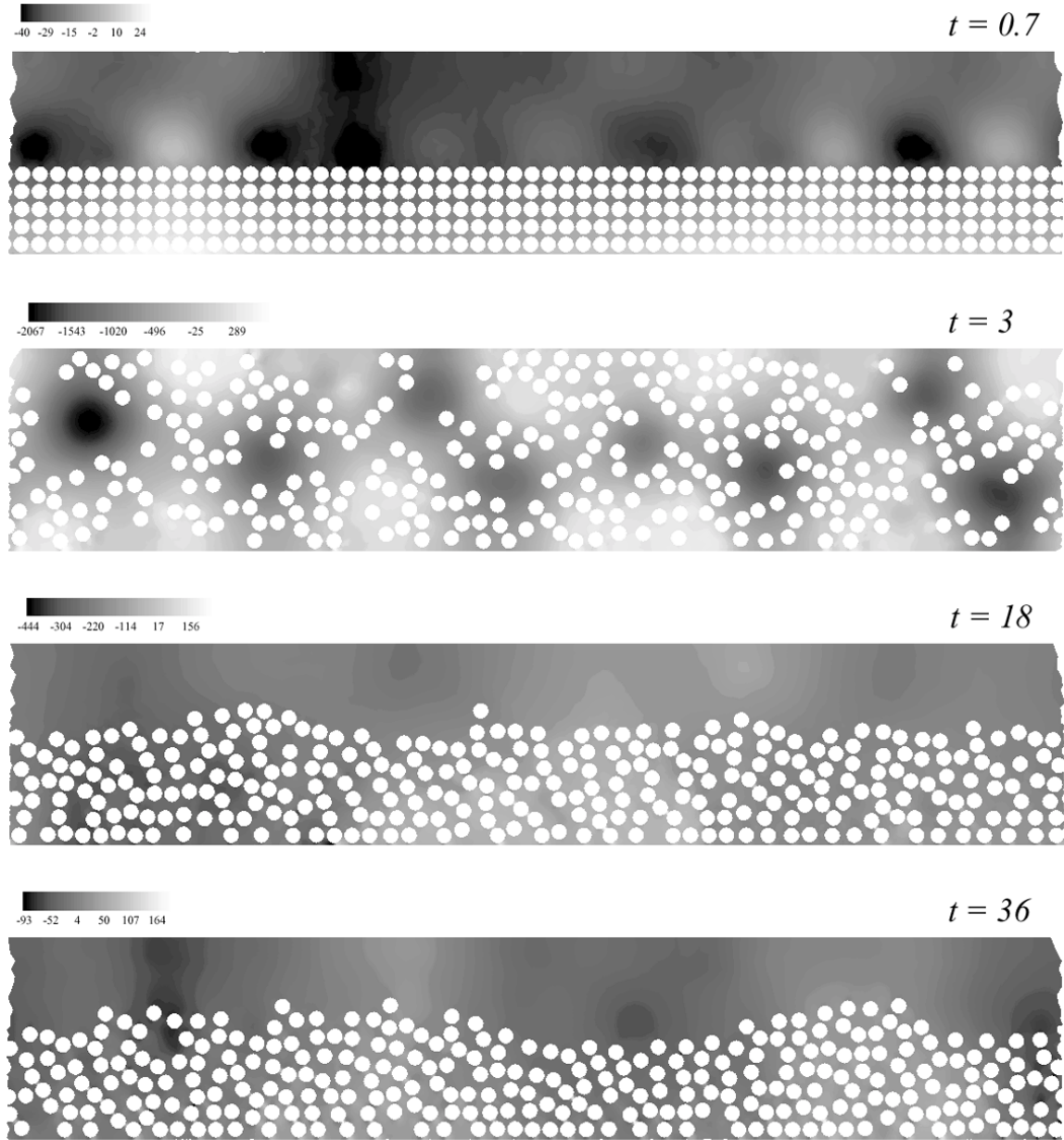


Figure 5.13. Fluidization of 300 particles ( $R_G = 3924$ ,  $R = 2400$ ).

Figure 6 shows the average height  $\bar{H}$  of the particle bed for the additional cases reported here. We observe that the increase in  $\bar{H}$  is monotonous at lower shear Reynolds numbers. The graph of  $\bar{H}$  eventually levels off to a constant steady value. At higher shear Reynolds numbers ( $R > 300$ ) there is an overshoot in the bed height during the transient. At sufficiently high shear Reynolds numbers the overshoot is large enough for

the particles to occupy the entire channel during the transient (Figures 4, 5.6, 5.7, 5.10-5.13). The bed finally settles to the steady equilibrium height. The amplitude of the waves formed on the fluid-mixture interface increases during the transient to cause bed erosion. At high shear Reynolds numbers the interfacial waves are more unstable resulting in the waves reaching the upper wall of the channel. The average lift on the particles increases with the particle fraction. At the peak height the average lift on the particles is not sufficient. Hence, they settle to a lower equilibrium height with larger particle fraction resulting in greater average lift. Another interpretation is that the shear at the top wall drives the particles near it towards the channel center thus reducing the average height (CJ).

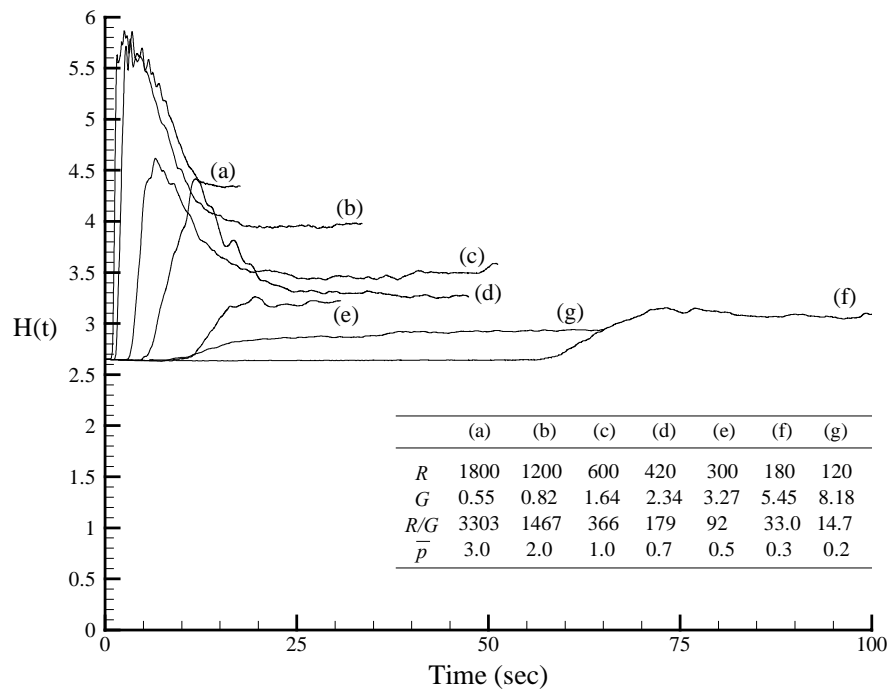


Figure 6.1. Rise curves for the average height of 300 circular particles fluidized by lift ( $\eta = 0.1$  poise,  $R = 600 \bar{p}$ ,  $R_G = 981$ ,  $\bar{p}$  is in dynes/cm<sup>2</sup>). Notice the overshoot at early times. The final bed height is an increasing function of  $\bar{p}$ . The bed at steady state when the rise curve levels off.

The time to steady state is longer when the Reynolds number is smaller.

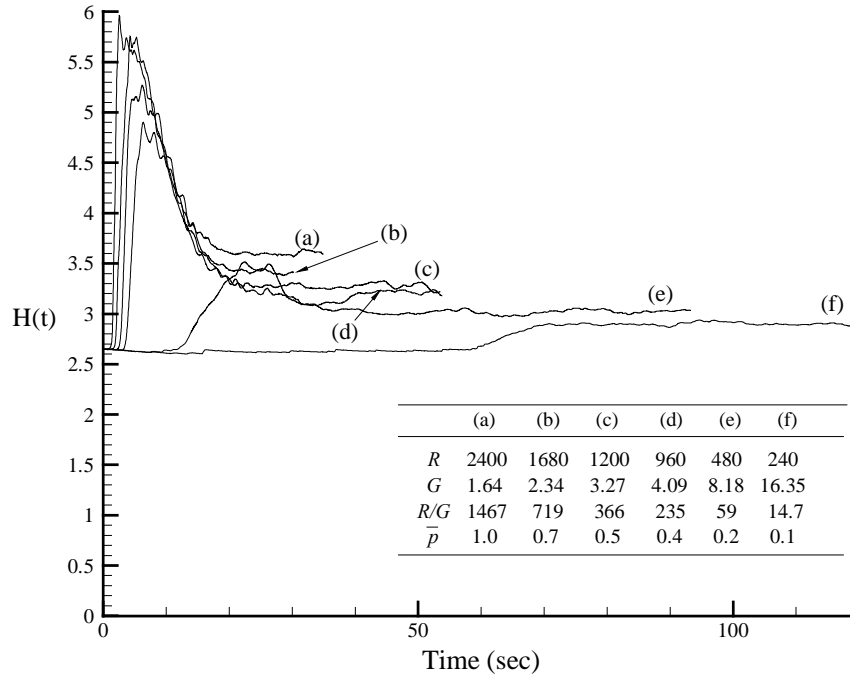


Figure 6.2. Rise curves for the average height of 300 circular particles fluidized by lift  
( $\eta = 0.05$  poise,  $R = 2400 \bar{p}$ ,  $R_G = 3924$ ,  $\bar{p}$  is in dynes/cm<sup>2</sup>).

Figure 5 shows that in the final state there are internal pressure waves which propagate horizontally. The pressure waves cause compression and rarefaction in the particle bed when the average equilibrium height is large. The waves of horizontal stratification of the particle fraction propagate with the pressure wave. Similar observations were reported by CJ. At lower values of the equilibrium height, the particles are close to one another and cannot be pushed together without driving some vertically upwards. This results in waves on the fluid-mixture interface, similar to those formed during the initial transient, which propagate with the pressure waves. In contrast to the waves formed during the transient phase, the waves in the final state are smaller in amplitude and do not grow.

Wave formation in sediment transport by water has been observed before in various scenarios (Kennedy 1969, Graf 1971, Bagnold 1973). Wind generated ripples and dunes were discussed by Bagnold (1941). Wavelike motion in pneumatic transport was studied



by Wen & Simons (1959) and Tomita, Jotaki & Hayashi (1981) among others. Wavelike slugs which resemble solitary waves in an open channel are observed in pneumatic transport (Wen & Simons 1959). Similar plugs are observed during the transient phase in our simulations (Figure 5.4,  $t = 12$ s). The plug is unstable and eventually breaks to settle to the final equilibrium height. Three different modes of transport of particles in water have been observed (Abbott & Francis 1977) – rolling, saltation and suspension. Kern, Perkins & Wyant (1959) reported similar modes for proppant transport in fractured reservoirs. All these modes are observed in our simulations. We observe rolling when the bed is not eroded at low Reynolds numbers. Waves are observed during the initial transient and the final steady state at relatively low equilibrium heights (Figure 5). The suspension of particles without interfacial waves is observed when the particle fraction at steady state is low (Figures 5.6 & 5.7).

Previous investigations of the fluidization of many particles by shear have focused on the creeping flow limit (see Morris & Brady 1998 and references therein) and on particle dispersion due to turbulence (Bagnold 1941, Graf 1971). In the creeping flow limit the hydrodynamic interaction between the particles tend to disperse them into regions of lower concentrations. This shear induced diffusivity balances gravitational settling. In turbulent flows, the solids are suspended against gravity by random eddy currents. The results of our simulations are valid for a range of Reynolds numbers.

The maximum value of  $R$  in our simulations is 2400 (Figure 5.13). We can also define a Reynolds number  $R_W = \rho_f V_{max} W / \eta$  based on the channel width, where  $V_{max}$  is the maximum velocity in the channel. For the case depicted in Figure 5.13,  $R_W = 86400$  if  $V_{max}$  is the maximum velocity in the absence of the particles whereas  $R_W = 14640$  for the same case if  $V_{max}$  is obtained from the simulation. The length scale (channel width) used in defining the Reynolds number  $R_W$  may be inappropriate. More appropriate length scale could be the spacing between the particles in the particle bed or the height of the clear fluid region in the upper part of the channel. Using height of the clear fluid region as the

length scale, the calculated Reynolds number for the case in Figure 5.13 is 5490. One might expect results, unlike those from our simulations, with turbulent flow features at these Reynolds numbers. The effect of large particles on fluid turbulence at high particle fractions is not well understood. Particles can enhance or suppress turbulence. It has been suggested that large particles can cause enhancement of turbulence due to wake shedding (Hetsroni 1989). In our simulations wake shedding is not significant (Figure 5). The difference between the average fluid and particle velocities (slip velocity) is very small (also see CJ). The presence of the particles increases the resistance to the flow; this increased resistance can be interpreted as an increase of apparent viscosity. This may lead to turbulence suppression in cases such as in our simulations where the particle fraction is relatively high. However, the upper part of the channel is often free from particles and not subjected to turbulence suppression. The lack of turbulence there may be an effect of two-dimensionality.

### ***3.2 Correlation for lift-off***

We obtain a correlation for the average equilibrium height of the particles based on the data from our simulations and those reported by CJ. Since  $W/d$  and  $Nd/l$  (or  $\varepsilon_{max}$ ) are fixed, the gravity Reynolds number  $R_G$  is a function of  $R$  and  $\varepsilon$ .

The effective weight of a particle in a suspension is  $(\pi d^2/4)(\rho_p - \rho_c)g = \varepsilon(\pi d^2/4)(\rho_p - \rho_f)g$  (Foscolo & Gibilaro 1984, Joseph 1990), where  $\rho_c$  is the effective or composite density of the fluid-particle mixture. Consequently, the net buoyant weight (or lift)  $L_s$  on a particle in a suspension is given by

$$L_s = \varepsilon L = \varepsilon(\pi d^2/4)(\rho_s - \rho_f)g. \quad (5)$$

We therefore plot  $\varepsilon R_G$  vs.  $R$  in Figure 7 at different values of fluid viscosities. At a given viscosity the value of  $R_G$  is a constant in our simulations. The fluid fraction or the equilibrium height of the particle bed increases as the shear Reynolds number is increased. Heavier particles are lifted to a smaller equilibrium height at the same shear

Reynolds number. We observe that the data at each viscosity (or  $R_G$ ) can be represented by a power law equation of the form  $\varepsilon R_G = cR^m$ , where the values of  $c$  and  $m$  are given in the figure. The value of  $c$  varies significantly with respect to  $R_G$  whereas the value of  $m$  does not show large variation. Figure 8 shows the plot of  $c$  vs.  $R_G$  on a logarithmic scale. The functional dependence of  $c$  on  $R_G$  is represented in terms of a power law equation. Combining this result with that in Figure 7 we can arrive at a correlation for  $R_G$  as a function of  $R$  and  $\varepsilon$ . In Figure 9 we reduce all the data points to a single curve. The prefactor in the expression for  $c$  is changed from 0.368 in Figure 8 to 0.4119 in Figure 9 for better agreement between the data and the correlation. The average value of the exponent  $m$  is also obtained from the curve fit for all the data points. We obtain the following correlation for  $R_G$  as a function of  $R$  and  $\varepsilon$

$$\begin{aligned}
 R_G &= 3.27 \times 10^{-4} \varepsilon^{-9.05} R^{1.249} \\
 \Rightarrow \varepsilon R_G &= 3.27 \times 10^{-4} \varepsilon^{-8.05} R^{1.249}.
 \end{aligned} \tag{6}$$

The data from which the correlation is derived had the following range of parameters:  $\varepsilon$  between 0.29 and 0.69,  $R_G$  ranging from 9.81 to 3924 and  $R$  ranging from 5.4 to 2400. It is well-known that particles sedimenting in a suspension experience greater drag at higher particle fractions. Similar behavior is observed for the hydrodynamic lift force on particles in a suspension (6).

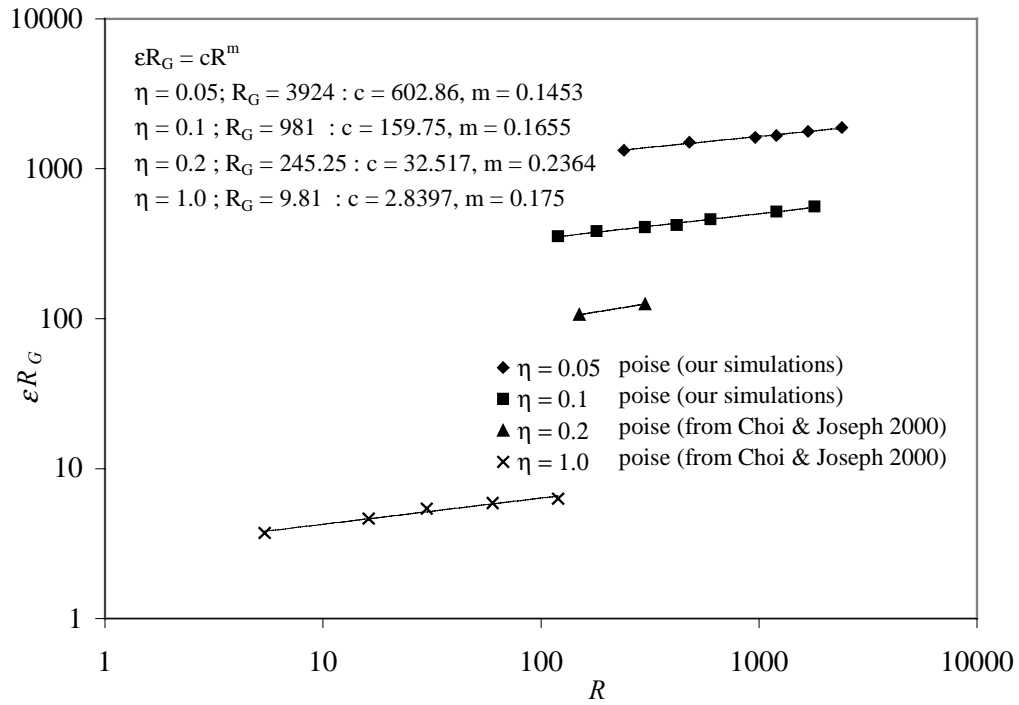


Figure 7. The plot of  $\varepsilon R_G$  vs. the shear Reynolds number  $R$  on a logarithmic scale for 300 particles in plane Poiseuille flows of Newtonian fluids at different values of fluid viscosities (or  $R_G$ ).

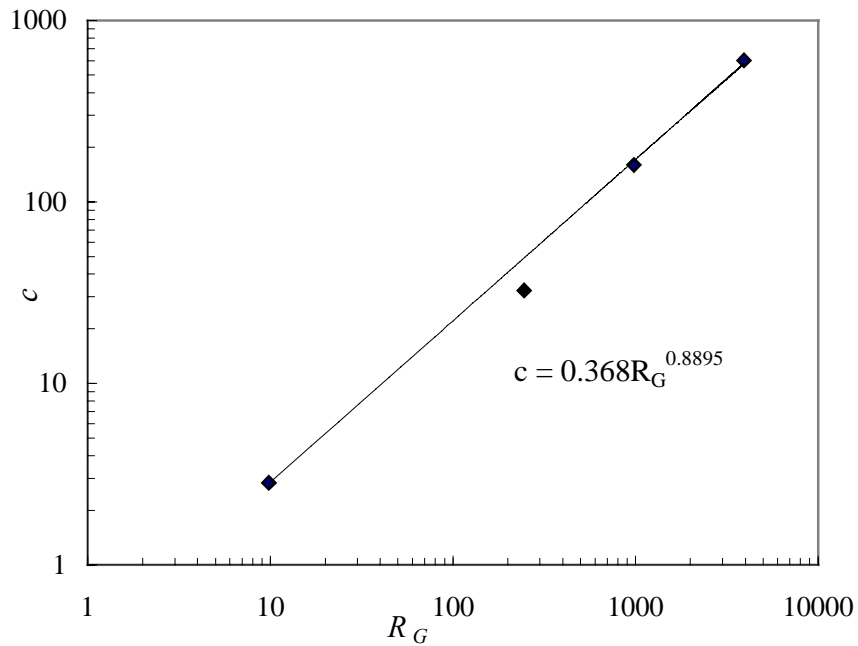


Figure 8. The plot of  $c$  vs.  $R_G$  on a logarithmic scale.

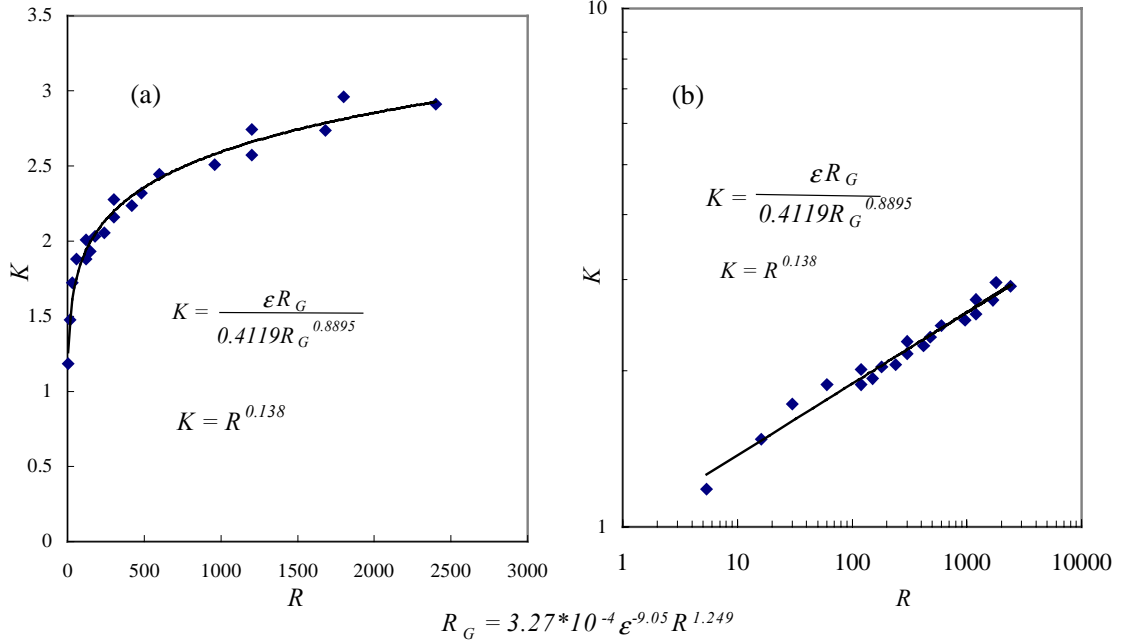


Figure 9. Correlation for lift-off from numerical simulations of 300 circular particles in plane Poiseuille flows of Newtonian fluids ( $W/d = 12$ ). (a) Regular scale (b) Logarithmic scale.

The ratio  $2\bar{H}/W$  denotes the fraction of the channel width occupied by the fluid-particle mixture. The correlation can be rewritten in terms of this parameter as

$$R_G = 3.27 \times 10^{-4} \left( \frac{(2\bar{H}/W) - \phi_{\min}}{2\bar{H}/W} \right)^{-9.05} R^{1.249}. \quad (7)$$

The correlation in dimensional form is

$$\bar{p} = 1234.88 \left( 1 - \frac{N\pi d^2}{8\bar{H}l} \right)^{7.25} \frac{\rho_f g^{0.8} \left( \frac{\rho_p}{\rho_f} - 1 \right)^{0.8} d^{0.4} \nu^{0.4}}{W}, \quad (8)$$

where,  $\nu$  is the kinematic viscosity of the fluid. The effect of  $W/d$  and  $\varepsilon_{max}$  on the correlation is not investigated.

The lift-off correlation above is valid for the average behavior of the suspension in a channel. It accounts for the effect of the Reynolds number on the lift-off of many particles. A similar correlation may also be developed based on the experimental data.

The correlation can be used to estimate the critical Reynolds number for lift-off of suspensions in a channel (for the given values of  $W/d$  and  $\varepsilon_{max}$ ). Let  $2\bar{H}_o$  be the initial height of the closely packed particle bed. Equation (7) implies

$$\frac{(2\bar{H}/W) - \phi_{min}}{2\bar{H}/W} = \left( \frac{3.27 \times 10^{-4} R^{1.249}}{R_G} \right)^{1/9.05} \stackrel{def}{=} C. \quad (9)$$

It follows that

$$\frac{2\bar{H}}{W} = \frac{\phi_{min}}{1-C}.$$

For fluidization, we have  $\bar{H} \geq \bar{H}_o$  where the equality represents the critical condition for lift-off. We also have

$$\phi_{max} = \frac{\pi d^2 N / 4}{2\bar{H}_o l}, \quad (10)$$

where,  $\phi_{max}$  is the particle fraction in the initial closely packed configuration and  $\phi_{min}$  is given in (4) as

$$\phi_{min} = \frac{\pi d^2 N / 4}{W l} = \frac{2\bar{H}_o}{W} \phi_{max}. \quad (11)$$

The condition for lift-off is then given by

$$\frac{2\bar{H}}{W} = \frac{\phi_{min}}{1-C} \geq \frac{2\bar{H}_o}{W}.$$

After replacing  $\phi_{min}$  with  $\phi_{max}$ , using (11), we find

$$\frac{2\bar{H}_o}{W} \frac{\phi_{max}}{1-C} \geq \frac{2\bar{H}_o}{W};$$

Hence

$$C \geq 1 - \phi_{max}. \quad (12)$$

Combining now (9) and (12) we get

$$R \geq \left( \frac{R_G}{3.27 \times 10^{-4}} [1 - \phi_{max}]^{9.05} \right)^{1/1.249},$$

where equality represents the critical shear Reynolds number  $R_{cr}$  for the lift-off of particles from the bed.

The correlation can also be used to estimate the smallest shear Reynolds number  $R_{cf}$  at which the particles would occupy the entire channel width at steady state ( $2\bar{H} = W$ ). Following steps similar to those in (12) we get

$$R_{cf} = \left( \frac{R_G}{3.27 \times 10^{-4}} [1 - \phi_{\min}]^{9.05} \right)^{1/1.249}. \quad (13)$$

It cannot be predicted with certainty that the particles will occupy the entire channel width at this Reynolds number. The effect of the upper wall may prevent such a possibility. The estimated value of  $R_{cf}$  may also be within the turbulent regime.

N. Patankar *et al.* (2001) obtained a correlation for the critical condition for lift-off of a single circular particle in a plane Poiseuille flow of a Newtonian fluid. They assumed a surface roughness of  $0.001d$  and defined the critical condition as the minimum shear Reynolds number required to lift a particle to an equilibrium height greater than  $0.501d$ . Their correlation is given by

$$R_{cr,1} = \left( \frac{R_G}{2.36} \right)^{1.39}, \quad (14)$$

where  $R_{cr,1}$  is the critical shear Reynolds number for lift-off of a single particle. Equation (14) is valid for  $W/d \geq 12$ .

Table 1 compares  $R_{cr}$  and  $R_{cr,1}$  for the values of  $R_G$  listed in Figure 7. In our simulations we had  $\phi_{\max} = 0.71$  and  $\phi_{\min} = 0.31$ . The values of  $R_{cf}$  are also listed.

$R_G$	$R_{cr}$	$R_{cr,1}$	$R_{cf}$
9.81	0.461	2.787	256.62
245.25	6.061	28.24	3377.06
981	18.39	76.56	10246.4
3924	55.80	207.56	31088.9

*Table 1. Comparison between the critical Reynolds numbers for lift-off of many particles and a single particle at different values of  $R_G$ . The smallest shear Reynolds numbers at which the particles would occupy the entire channel width at steady state are also listed.*

The shear Reynolds numbers in our computations are between  $R_{cr}$  and  $R_{cf}$  at all values of  $R_G$ . Due to the computational cost, many particle simulations were not performed to

confirm the value of  $R_{cr}$  estimated from the correlation. The average bed height did not increase after a long computation when the shear Reynolds number was less than  $R_{cr}$  for some cases we tested. Table 1 shows that the critical shear Reynolds number for lift-off of a single particle is greater than that for many particles at the same value of  $R_G$ . This is similar to the fluidization of particles by drag where the critical velocity for fluidization of a single particle is more than that for many particles.

Previous investigation by Morris & Brady (1998) addresses the problem of lift-off of many particles in the creeping flow limit. They considered the balance between gravitational settling and Fickian diffusion of particles. The diffusivity in their simulations was the shear-induced diffusivity driven by hydrodynamic interactions between the particles. In their analysis the average height of the particle bed depends on a dimensionless parameter  $B$  characterizing the relative strength of buoyancy to shearing. It can be verified that their parameter  $B \sim O\left(R_G W / Rd\right)$ . Therefore, in the creeping flow limit,  $R_G / R = f\left(\varepsilon, Nd/l, W/d\right)$  instead of the general form at finite Reynolds numbers in (4). At finite Reynolds numbers, inertia plays a role in the balance of the buoyant weight and the hydrodynamic lift on the particles.

Models for the drag force on particles in solid-liquid mixtures, which rely on the well-known Richardson-Zaki (1954) correlation, are usually obtained in terms of the single particle drag formula, Reynolds number and the fluid fraction. Reduction of the lift-off correlation in (6) in terms of the single particle lift formula is not straightforward. This is because, more than one equilibrium positions are possible for a single particle in a channel (CJ, N. Patankar *et al.* 2001). N. Patankar *et al.* (2001) have identified this as a double turning point solution. We have not observed multiple equilibrium heights of the particle bed in our many particle simulations.



#### 4. Conclusions

1. 2D numerical simulations of the lift-off of 300 circular particles in plane Poiseuille flows of Newtonian fluids are performed.
2. Lift-off is initiated by the formation of horizontal pressure waves and the corresponding waves at the fluid-mixture interface.
3. At low shear Reynolds numbers, there is a monotonous increase of the average height of the particle bed to the final equilibrium value.
4. At higher shear Reynolds numbers ( $R > 300$ ) there is an overshoot in the bed height, with particles sometimes occupying the entire channel width, during the transient. The bed finally settles to a lower equilibrium height for the cases considered here.
5. In the final state there are internal pressure waves which propagate horizontally. There are corresponding waves in the particle bed.
6. The average fluid fraction of the particle bed increases as the shear Reynolds number is increased. Heavier particles are lifted to a smaller equilibrium height at the same Reynolds number.
7. A correlation for the lift-off of many particles in 2D is obtained from the numerical data modeling procedures to be used in getting correlations that we think will emerge from 3D simulations presently under way.
8. The correlation is used to estimate the critical shear Reynolds number for lift-off of many particles and the smallest shear Reynolds number at which the particles would occupy the entire channel width at steady state.
9. The critical shear Reynolds number for lift-off of a single particle is greater than that for many particles at the same value of  $R_G$ . This is similar to the fluidization of particles by drag where the critical velocity for fluidization of a single particle is more than that for many particles.

## Acknowledgment

This work was partially supported by the National Science Foundation KDI/New Computational Challenge grant (NSF/CTS-98-73236), by the US Army, Mathematics, by the DOE, Department of Basic Energy Sciences, by a grant from the Schlumberger foundation and from Stimlab Inc. and by the Minnesota Supercomputer Institute.

## References

- Abbott, J. & Francis, J. R. D. 1977 Saltation and suspension trajectories of solid grains in a water stream. *Philosophical Transactions of the Royal Soc. London Ser. A - Mathematical and Physical Sci.* **284**, 225-254.
- Bagnold, R. A. 1941 *The physics of blown sands and desert dunes*. Muthuen, London.
- Bagnold, R. A. 1973 The nature of saltation and of 'bed-load' transport in water. *Proc. Royal Soc. London Ser. A - Mathematical & Physical Sci.* **332**, 473-504.
- Choi, H. G. 2000 Splitting method for the combined formulation of fluid-particle problem, *Comput. Meth. Appl. Mech. Engrg.* **190**, 1367-1378.
- Choi, H. G. & Joseph, D. D. 2001 Fluidization by lift of 300 circular particles in plane Poiseuille flow by direct numerical simulation. *to appear, J. Fluid Mech.*
- Chorin, A. J. 1968 Numerical solution of the Navier-Stokes equations. *Math. Comput.* **22**, 745-762.
- Foscolo, P. V. & Gibilaro, L. G. 1984 A fully predictive criterion for transition between particulate and aggregate fluidization. *Chem. Engng. Sci.* **39**, 1667-1675.
- Graf, W. H. 1971 *Hydraulics of sediment transport*. McGraw Hill, New York.
- Hetsroni, G. 1989 Particle-turbulence interaction. *Int. J. Multiphase Flow* **15**, 735-746.
- Hu, H. H. 1996 Direct simulation of flows of solid-liquid mixtures. *Int. J. Multiphase Flow* **22**, 335-352.
- Hu, H. H., Joseph, D. D. & Crochet, M. J. 1992 Direct numerical simulation of fluid particle motions. *Theoret. Comput. Fluid Dynamics.* **3**, 285-306.

- Hu, H. H. & Patankar, N. A. 2001 Simulation of particulate flows in Newtonian and viscoelastic fluids, *to appear, International Journal of Multiphase Flow*.
- Hu, H. H., Patankar, N. A. & Zhu, M.-Y. 2001 Direct numerical simulations of fluid-solid systems using the Arbitrary-Lagrangian-Eulerian technique, *to appear, Journal of Computational Physics*.
- Joseph, D. D. 1990 Generalization of the Foscolo-Gibilaro analysis of dynamic waves. *Chem. Engng. Sci.* **45**, 411-414.
- Joseph, D. D. 2001 Interrogations of direct numerical simulation of solid-liquid flow, *submitted to Phys. Fluids*.
- Kennedy, J. F. 1969 The formation of sediment ripples, dunes & antidunes. *Ann. Rev. Fluid Mech.* **1**, 147-168.
- Kern, L. R., Perkins, T. K. & Wyant, R. E. 1959 The mechanics of sand movement in fracturing. *Petroleum Transactions, AIME.* **216**, 403-405.
- Ko, T., Patankar, N. A. & Joseph, D. D. 2001 A note on the lift-off of a single particle in viscoelastic fluids, *submitted to Phys. Fluids*.
- Morris, J. F. & Brady, J. F. 1998 Pressure-driven flow of a suspension: buoyancy effects. *Int. J. Multiphase Flow.* **24**, 105-130.
- Patankar, N. A., Huang, P. Y., Ko, T. & Joseph, D. D. 2001 Lift-off of a single particle in Newtonian and viscoelastic fluids by direct numerical simulation, *to appear, J. Fluid Mech.*
- Richardson, J. F. & Zaki, W. N. 1954 Sedimentation and fluidization: Part I. *Trans. Instn. Chem. Engrs.* **32**, 35-53.
- Tomita, Y., Jotaki, T. & Hayashi, H. 1981 Wavelike motion of particulate slugs in a horizontal pneumatic pipeline. *Int. J. Multiphase Flow.* **7**, 151-166.
- Wen, C. Y. & Simons, H. P. 1959 Flow characteristics in horizontal fluidized solids transport. *AIChE J.* **5**, 263-267.